

INCLUSIVE PRODUCTION OF NEUTRAL STRANGE PARTICLES  
IN 250 GeV/c  $\pi^-p$  INTERACTIONS\*

D. Bogert, R. Hanft, R. Harris, F.R. Huson, S. Kahn,<sup>‡</sup>  
C. Pascaud,<sup>†</sup> and W.M. Smart  
Fermi National Accelerator Laboratory,  
Batavia, Illinois 60510

and

J.R. Albright, S. Hagopian, P. Hays and  
J.E. Lannutti  
Florida State University,  
Tallahassee, Florida 32306

April 1977

ABSTRACT

Neutral strange particle production has been studied in a 46,000-picture exposure in the Fermilab 15-ft. bubble chamber. Cross sections for inclusive production of  $K_S^0$ ,  $\Lambda$ , and  $\bar{\Lambda}$  are given and compared with data at lower energies. The  $K_S^0$ 's are produced principally in the central region of rapidity with a cross section which increases with energy. The  $\Lambda$ 's are produced principally by proton fragmentation, whereas the  $\bar{\Lambda}$ 's are centrally produced. Correlations of  $K_S^0\pi^+$  and  $K_S^0K_S^0$  are shown to be different from those for  $\pi^-\pi^+$ .

\*Work supported in part by the U.S. Energy Research and Development Administration.

<sup>‡</sup>Present address: Brookhaven Nat. Laboratory, Upton, NY.

<sup>†</sup>Present address: Laboratoire de l'Accélérateur linéaire, Orsay, France.

This report presents results of a study of inclusive production of neutral strange particles at 250 GeV/c from the first experiment using hadrons in the Fermilab 15-foot bubble chamber. In this chamber the detection efficiencies for  $K_S^0$ 's,  $\Lambda$ 's and  $\bar{\Lambda}$ 's are higher than has been possible in previous experiments.

The data come from a 46,000-picture exposure of 250 GeV/c  $\pi^-p$  interactions. The film was scanned for all V's which could be candidates for  $K_S^0$ ,  $\Lambda$ , or  $\bar{\Lambda}$ , that is all V's with no identified electron. The scanning efficiency for such V's was 88%. The V's were measured and processed through the HYDRA geometry and kinematics programs. Kinematic fits were tried to  $K_S^0 \rightarrow \pi^-\pi^+$ ,  $\Lambda \rightarrow p\pi^-$ ,  $\bar{\Lambda} \rightarrow \bar{p}\pi^+$  and  $\gamma(p_S) \rightarrow e^+e^-(p_S)$ , where the last fit assumed a proton "spectator." The system efficiency to obtain some fit with at least a 1.5%  $\chi^2$ -probability was about 90%.

Approximately 68% of the V's fit two or more hypotheses. Ambiguities involving  $\gamma$ 's were resolved by comparing the momentum of the electron transverse to the  $\gamma$  direction,  $p_\perp$ , with a maximum value which was taken to depend upon the momentum of the  $\gamma$  as follows:  $p_{\perp\max} = 0.01 \text{ GeV/c} + 0.0013 p(\gamma)$  (with  $p(\gamma)$  in GeV/c) for  $p(\gamma) > 15 \text{ GeV}$ , or  $p_{\perp\max} = 0.025 \text{ GeV/c}$  for  $p(\gamma) < 15 \text{ GeV/c}$ . Thus V's with an opening angle near zero (with the criteria loosened where measuring errors were larger) were assumed to be  $\gamma$ 's. The losses of  $K_S^0$ ,  $\Lambda$ , and  $\bar{\Lambda}$  particles resulting from use of these criteria are estimated to be 0.6%, 1.5% and 2%, respectively, by comparing the  $p_\perp$

distributions with those predicted by assuming isotropic decay of the strange particles.

Ambiguities between  $K_S^0$ 's and  $\Lambda$ 's or  $\bar{\Lambda}$ 's were resolved by comparing the ratio of the probabilities of the two fits to a momentum-dependent function which is proportional to the ratio of unambiguous  $K_S^0$ 's to  $\Lambda$ 's (this favors  $\Lambda$ 's of low energy and  $K_S^0$ 's of high energy). The distribution of  $\cos\theta$ , where  $\theta$  is the center-of-mass angle between the direction of the V and one of its decay particles, is sensitive to the resolution of these ambiguities, and is found to be reasonably flat for  $K_S^0$ 's,  $\Lambda$ 's, and  $\bar{\Lambda}$ 's. The contaminations from strange particle ambiguities estimated from the  $\cos\theta$  plots are ~4% for  $K_S^0$ , ~5% for  $\Lambda$ , and ~10% for  $\bar{\Lambda}$ .

After resolving ambiguities, the number of events assigned to each category was 1059  $K_S^0$ 's, 427  $\Lambda$ 's and 103  $\bar{\Lambda}$ 's.

For calculating cross sections, a further cut was required to remove biases due to loss of V's close to the primary vertex and those lost in the forward jet. This criterion was determined by studying the lifetime distributions for the  $K_S^0$ 's,  $\Lambda$ 's, and  $\bar{\Lambda}$ 's. Reasonable results were obtained after requiring a minimum length for the neutral particle of 0.75 $\ell$  for  $K_S^0$ 's and 0.25 $\ell$  for  $\Lambda$ 's and  $\bar{\Lambda}$ 's, where  $\ell$ , in each case, is the respective mean decay-length in the lab. The final numbers of events used for cross section calculations are given in Table I.

Inclusive cross sections were obtained by weighting each V to correct for losses due to the minimum-length cut,

for those which decayed outside of the fiducial volume (a sphere of radius 1.6m), for V scanning efficiency ( $93 \pm 6\%$  after correction for the minimum-length cut), and for unseen neutral decay modes. No distinction was made between  $\Lambda$  and  $\Sigma^0$ , and the contribution from  $K_L^0$  was not included. The resulting cross sections for inclusive production of single and double V's are given in Table I.

Figure 1 shows the momentum dependence<sup>2</sup> of the inclusive cross sections for  $K_S^0$ ,  $\Lambda$ , and  $\bar{\Lambda}$ . The  $K_S^0$  and  $\bar{\Lambda}$  cross sections increase with momentum while the  $\Lambda$  cross section is approximately constant above 20 GeV/c.

The center-of-mass rapidity distributions for  $K_S^0$ 's,  $\Lambda$ 's, and  $\bar{\Lambda}$ 's are shown in Fig. 2. For the  $K_S^0$ 's, the rapidity distribution shown in Fig. 2a is consistent with the existence of a plateau of approximately two units symmetrically centered at zero. For comparison, the  $d\sigma/dy$  distribution at 100 GeV/c,<sup>2</sup> which is available only for  $y < 0$ , is also shown. It appears that the values in the central region of rapidity are approximately equal at 100 and 250 GeV/c.

Above 100 GeV/c, most models which include central region production predict a  $\ln s$  or  $(\ln s)^2$  increase in cross section. There is an expected  $\ln s$  increase due to the increase in the width of the rapidity plateau and another factor of  $\ln s$  if the plateau height increases like that seen for pions at the CERN ISR.<sup>1</sup> Although the rising cross section for  $K_S^0$ 's and the central rapidity plateau indicate central production, data on  $\sigma(K_S^0)$  as they stand are insufficient to allow

us to choose between the two alternatives of  $\ln s$  or  $(\ln s)^2$  dependence for  $\sigma(K_S^0)$ .

The  $d\sigma/dy$  distribution for  $\Lambda$ 's in Fig. 2b shows a maximum in the negative  $y$  region. This is as expected if most of the production is due to fragmentation of the target proton.<sup>3</sup> There is, however, significant production of  $\Lambda$ 's near  $y=0$ . This is to be compared with  $d\sigma/dy$  for  $\bar{\Lambda}$ 's, in Fig. 2c, which is approximately equal to  $d\sigma/dy$  for  $\Lambda$ 's at  $y=0$  and essentially symmetric about  $y=0$ . However, this does not necessarily imply the dominance of  $\Lambda\bar{\Lambda}$  pair production in this region since, as shown in Table I,  $\bar{\Lambda}$ 's are also produced with  $K_S^0$ 's.

The production of these particles can be further clarified by examining the relation between rapidities of pairs of strange particles. Fig. 3 shows scatterplots of the rapidity of one  $V$  versus that of the other  $V$  for the pairs  $K_S^0 K_S^0$ ,  $K_S^0 \Lambda$ ,  $K_S^0 \bar{\Lambda}$ , and  $\Lambda \bar{\Lambda}$ . To improve statistics the bias cuts used in the other figures of the paper have been ignored here. The  $K_S^0 K_S^0$  and the  $K_S^0 \bar{\Lambda}$  plots are denser in the center indicating strong central pair-production. The  $K_S^0 \Lambda$  plot shows roughly one-third central production ( $y_\Lambda > -1.0$ ), and a significant fraction of events with both  $y_\Lambda$  and  $y_{K_S^0}$  in the proton fragmentation region. The  $\Lambda \bar{\Lambda}$  plot shows mostly central-region pairs, but also has events with large negative  $\Lambda$  rapidity.

To investigate scaling, the invariant cross sections

$F_1(x)$  and  $F_2(p_{\perp}^2)$  are shown in Fig. 4, where

$$F_1(x) = \frac{2}{\pi\sqrt{s}} \int E^* \frac{d^2\sigma}{dx dp_{\perp}^2} dp_{\perp}^2$$

$$F_2(p_{\perp}^2) = \frac{2}{\pi\sqrt{s}} \int E^* \frac{d^2\sigma}{dx dp_{\perp}^2} dx$$

The  $F_1(x)$  distributions are compared with data at 18.5 GeV/c<sup>1</sup> in Figs. 4a, 4b, and 4c. The distributions for  $K_S^0$  and  $\bar{\Lambda}$  do not scale; the  $K_S^0$  distributions differ in shape, while the  $\bar{\Lambda}$  distributions differ in magnitude. Although the  $\Lambda$  distribution does appear to scale, this may be fortuitous since a significant fraction of the cross section at  $x=0$  can be attributed to  $\Lambda\bar{\Lambda}$  production at 250 GeV/c, whereas this is certainly not true at 18.5 GeV/c.

The  $F_2(p_{\perp}^2)$  distributions in Fig. 4d have been fitted to simple exponentials over the region  $0 < p_{\perp}^2 < 1 (\text{GeV}/c)^2$ , yielding slopes of  $(3.2 \pm 0.3) (\text{GeV}/c)^{-2}$ ,  $(3.0 \pm 0.3) (\text{GeV}/c)^{-2}$  and  $(2.5 \pm 0.6) (\text{GeV}/c)^{-2}$  for  $K_S^0$ 's,  $\Lambda$ 's, and  $\bar{\Lambda}$ 's, respectively. The slope for  $\Lambda$ 's is slightly larger than that for  $\bar{\Lambda}$ 's, as might be expected, since  $\Lambda$  production has been shown to be primarily via fragmentation, which results in smaller average  $p_{\perp}^2$ . There is some evidence in Fig. 4d that the  $\Lambda$  distribution is steeper at small  $p_{\perp}^2$  than at large  $p_{\perp}^2$ .

The correlation between neutral strange-particle production and charged  $\pi$ 's can be seen in the dependence of the average number of V's,  $\langle n_V \rangle$ , with charged multiplicity, as shown in Table II and Fig. 5. The  $\langle n_{K_S^0} \rangle$  distribution

seems to exhibit a distinct rise with multiplicity similar to that seen for  $\pi^0$  production.<sup>1</sup> This effect is not as obvious in lower energy  $\pi p$  experiments,<sup>4</sup> which are consistent with  $\langle n_{K_S^0} \rangle$  being constant with multiplicity. The  $\langle n_\Lambda \rangle$  distribution is consistent with being constant with respect to multiplicity above  $n=4$ , as would be expected since target fragmentation dominates  $\Lambda$  production.

To study the differences in correlations between  $\pi$ 's and  $K$ 's, we have calculated the correlation function  $R(\Delta y)$ , where  $\Delta y = y_2 - y_1$  and

$$R(y_1, y_2) = \frac{\rho_{12}(y_1, y_2)}{\rho_1(y_1)\rho_2(y_2)} - 1$$

$$\rho_{12} = \frac{1}{\sigma_{inel}} \frac{d^2\sigma}{dy_1 dy_2} \qquad \rho_1 = \frac{1}{\sigma_{inel}} \frac{d\sigma}{dy_1}$$

in which  $\rho_{12}$ ,  $\rho_2$  and  $\rho_1$  are the double and single rapidity densities.  $R(\Delta y)$  was obtained by integrating  $R(y_1, y_2)$  with respect to  $y_1$  and  $y_2$  over the region  $-2 < y_2 < 2$ ,  $-2 < y_1 < 2$ . This function is shown for  $\pi^-\pi^+$ ,  $K_S^0 \pi^+$  and  $K_S^0 K_S^0$  pairs in Fig. 6. Here " $\pi$ " includes all charged particles except identified protons. The  $R(\pi^-\pi^+)$  distribution is in good agreement with an experiment at 205 GeV/c which has better statistics.<sup>5</sup> The  $K_S^0 \pi^+$  pairs show smaller correlation than  $\pi^-\pi^+$ , while the  $K_S^0 K_S^0$  pairs show a significantly larger correlation at  $\Delta y=0$ .

In conclusion, we have shown that  $K_S^0$ 's are produced predominantly in the central region, with a cross section which increases with energy. The  $\langle n_{K_S^0} \rangle$  exhibits an increase with multiplicity and  $K_S^0 K_S^0$  pairs show a strong correlation at  $\Delta y=0$ . All this is qualitatively similar to what is known about the production of charged and neutral  $\pi$ 's. The production of  $\Lambda$ 's is mostly associated with the fragmentation of the proton, whereas, the  $\bar{\Lambda}$ 's are centrally produced.

We appreciate the support given to us by the Fermilab beam and bubble chamber crews during the pioneering 15-foot bubble chamber run. We are grateful to the scanning staffs at both labs. We would like to thank R. Bates, M. Harrison, and M. Sokoloff for help in the analysis, and J.F. Owens for useful comments.

## REFERENCES

1. J. Whitmore, Phys. Lett. 27C, 187 (1976).
2. 11.5 GeV/c: T. Ferbel and H. Taft, Nuovo Cimento 28, 1214 (1963).
- 16 GeV/c: J. Bartke, et al., Nuovo Cimento 24, 876 (1962).
- 18.5 GeV/c: P.H. Stuntebeck, et al., Phys. Rev. D9, 608 (1974).
- 20 GeV/c: E. Balea, et al., Rev. Roumanian Phys. 15, 587 (1970).
- 40 GeV/c: E. Balea, et al., Nucl. Phys. B79, 57 (1974).
- 100 GeV/c: E.L. Berger, et al., CERN/D. PhII/PHYS 74-27 (1974).
- 147 GeV/c: T. Watts, private communication.
- 205 GeV/c: D. Ljung, et al., to be published.
3. It is also interesting that J.F. Owens has been able to predict the magnitude and momentum dependence of  $\sigma(\Lambda)$  covered in Figure 1 using a pure fragmentation model with no free parameters (private communication).
4. S. Kahn, in H.J. Lubatti, and P.M. Mockett, eds. Particles and Fields 1975 (University of Washington, Seattle, 1975), p. 292.
5. N.N. Biswas, et al., Phys. Rev. Lett. 35, 1059 (1975).
6. There were 12 events with 3 observed V's and one 4V event. After applying the bias cut, only 3 of the 3V events remained. Events observed were: four  $K_S^0 K_S^0 K_S^0$ , six  $K_S^0 K_S^0 \Lambda$ , two  $K_S^0 \Lambda \bar{\Lambda}$ , and one  $K_S^0 K_S^0 K_S^0 \Lambda$ .

TABLE I

## Inclusive Cross Sections

<u>Reaction</u>	<u>Cross Section (mb)</u>	<u>No. of Events</u>
$\pi^- p \rightarrow K_S^0 + X$	$3.98 \pm 0.5$	624
$\rightarrow \Lambda + X$	$1.47 \pm 0.2$	362
$\rightarrow \bar{\Lambda} + X$	$0.41 \pm 0.09$	82
$\rightarrow K_S^0 K_S^0 + X$	$0.62 \pm 0.2$	30
$\rightarrow K_S^0 \Lambda + X$	$0.41 \pm 0.1$	30
$\rightarrow K_S^0 \bar{\Lambda} + X$	$0.13 \pm 0.06$	7
$\rightarrow \Lambda \bar{\Lambda} + X$	$0.15 \pm 0.06$	9
$\rightarrow \Lambda \Lambda + X$	$0.04 \pm 0.02$	5
$\rightarrow (\geq 3V) + X$	(see Ref. 6)	

TABLE II

## Multiplicity Dependence of Strange Particle Production

<u>K<sub>S</sub><sup>0</sup></u>				<u>Λ</u>			<u>Λ̄</u>		
No. of Prongs	No. of K <sub>S</sub> <sup>0</sup> 's	σ (mb)	<n <sub>K<sub>S</sub><sup>0</sup></sub> >	No. of Λ's	σ (mb)	<n <sub>Λ</sub> >	No. of Λ̄'s	σ (mb)	<n <sub>Λ̄</sub> >
0	2	0.11±0.008	0.85±0.7	2	0.007±0.005	0.54±0.4	0	-	-
2	17	0.11±0.03	0.06±0.02	13	0.05±0.01	0.024±0.008	2	0.01±0.01	0.007±0.006
4	47	0.31±0.05	0.10±0.02	39	0.14±0.02	0.045±0.007	5	0.02±0.01	0.008±0.004
6	106	0.66±0.07	0.17±0.02	71	0.28±0.03	0.071±0.009	19	0.09±0.02	0.025±0.006
8	118	0.76±0.07	0.20±0.02	70	0.30±0.04	0.08±0.01	16	0.08±0.02	0.019±0.005
10	100	0.64±0.07	0.20±0.02	62	0.26±0.04	0.08±0.01	20	0.11±0.03	0.033±0.008
12	102	0.66±0.07	0.29±0.03	46	0.19±0.03	0.08±0.01	7	0.03±0.01	0.013±0.005
14	66	0.39±0.05	0.28±0.04	28	0.12±0.02	0.08±0.02	5	0.03±0.01	0.019±0.009
16	27	0.17±0.03	0.23±0.05	12	0.05±0.01	0.06±0.02	2	0.007±0.005	0.010±0.007
18	22	0.12±0.03	0.38±0.07	5	0.019±0.009	0.05±0.02	2	0.01±0.01	0.04±0.03
20	10	0.06±0.02	0.30±0.1	9	0.04±0.01	0.19±0.07	2	0.01±0.01	0.07±0.05
>20	7	0.05±0.02	0.40±0.18	5	0.03±0.01	0.30±0.14	2	0.008±0.005	0.30±0.2
TOTAL	624	3.98±0.5	0.19±0.02	362	1.47±0.2	0.070±0.008	82	0.41±0.09	0.020±0.003

## FIGURE CAPTIONS

- Figure 1 - Inclusive production cross sections for  $K_S^0$ ,  $\Lambda$ , and  $\bar{\Lambda}$  as a function of laboratory momentum. Data for other momenta obtained as given in Reference 1.
- Figure 2 -  $d\sigma/dy$  center-of-mass rapidity distributions for: (a)  $K_S^0$ 's; (b)  $\Lambda$ 's; (c)  $\bar{\Lambda}$ . For  $d\sigma(K_S^0)/dy$ , the distribution for 100 GeV/c for  $y < 0$  is also given for comparison.
- Figure 3 - Scatterplots of the rapidity of  $V_1$  versus the rapidity of  $V_2$  in double-V events: (a)  $K_S^0 K_S^0$  (plotted with  $y(K_1) > y(K_2)$ ), (b)  $K_S^0 \Lambda$ , (c)  $K_S^0 \bar{\Lambda}$ , and (d)  $\Lambda \bar{\Lambda}$ .
- Figure 4 - Invariant function  $F_1(x)$  is given for: (a)  $K_S^0$ 's; (b)  $\Lambda$ 's; (c)  $\bar{\Lambda}$ 's. For comparison, data for 18.5 GeV/c is also given with the  $F_1(x)$  distributions. (d) gives the invariant function  $F_2(p_{\perp}^2)$  for  $K_S^0$ 's,  $\Lambda$ 's and  $\bar{\Lambda}$ 's.
- Figure 5 - Average number of  $K_S^0$ 's,  $\Lambda$ 's, and  $\bar{\Lambda}$ 's as a function of the number of charged prongs.
- Figure 6 - Correlation function  $R(\Delta y)$ , defined in the text, for particle pairs  $\pi^+ \pi^-$ ,  $K_S^0 \pi^+$ , and  $K_S^0 K_S^0$ .

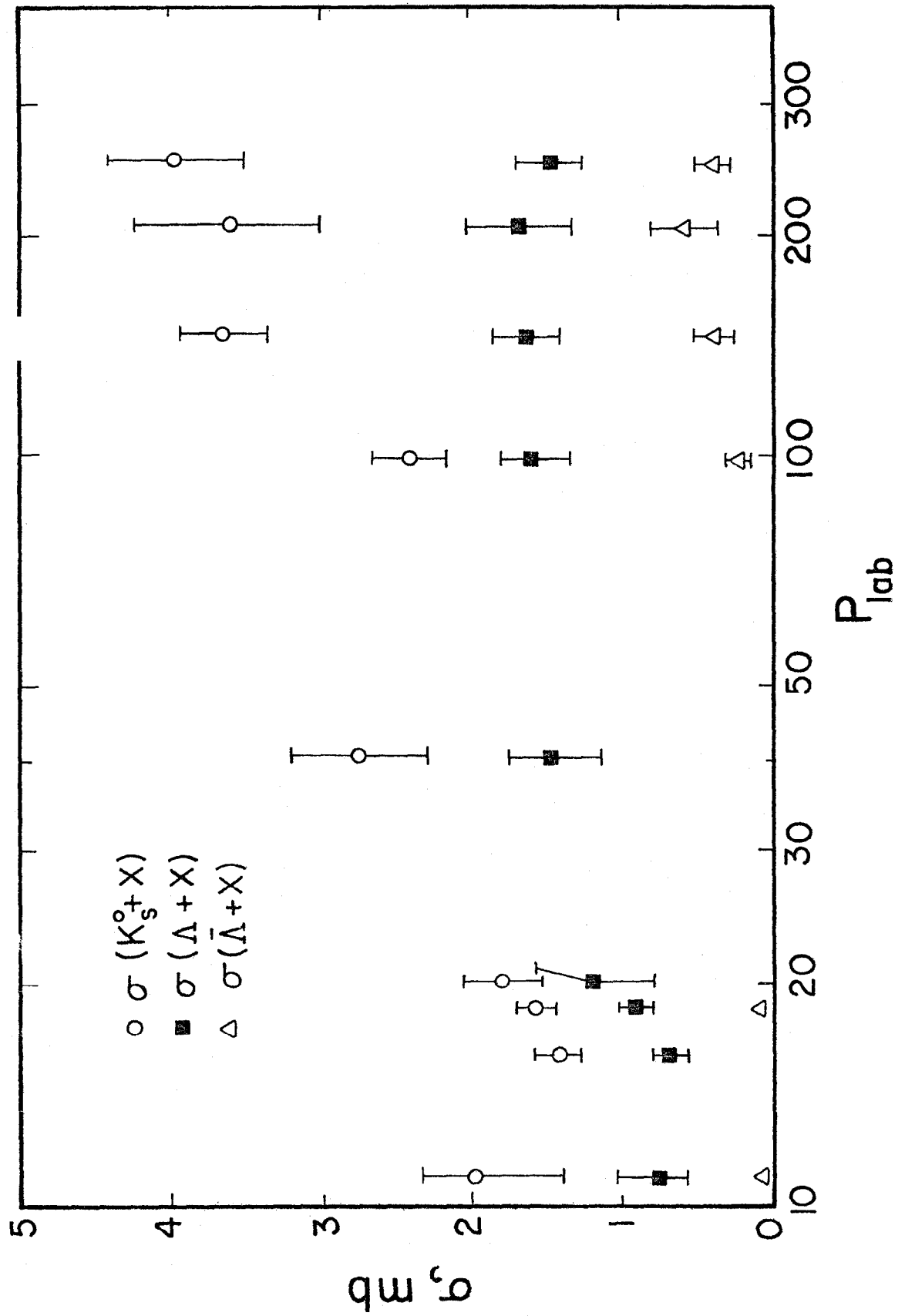


Figure 1

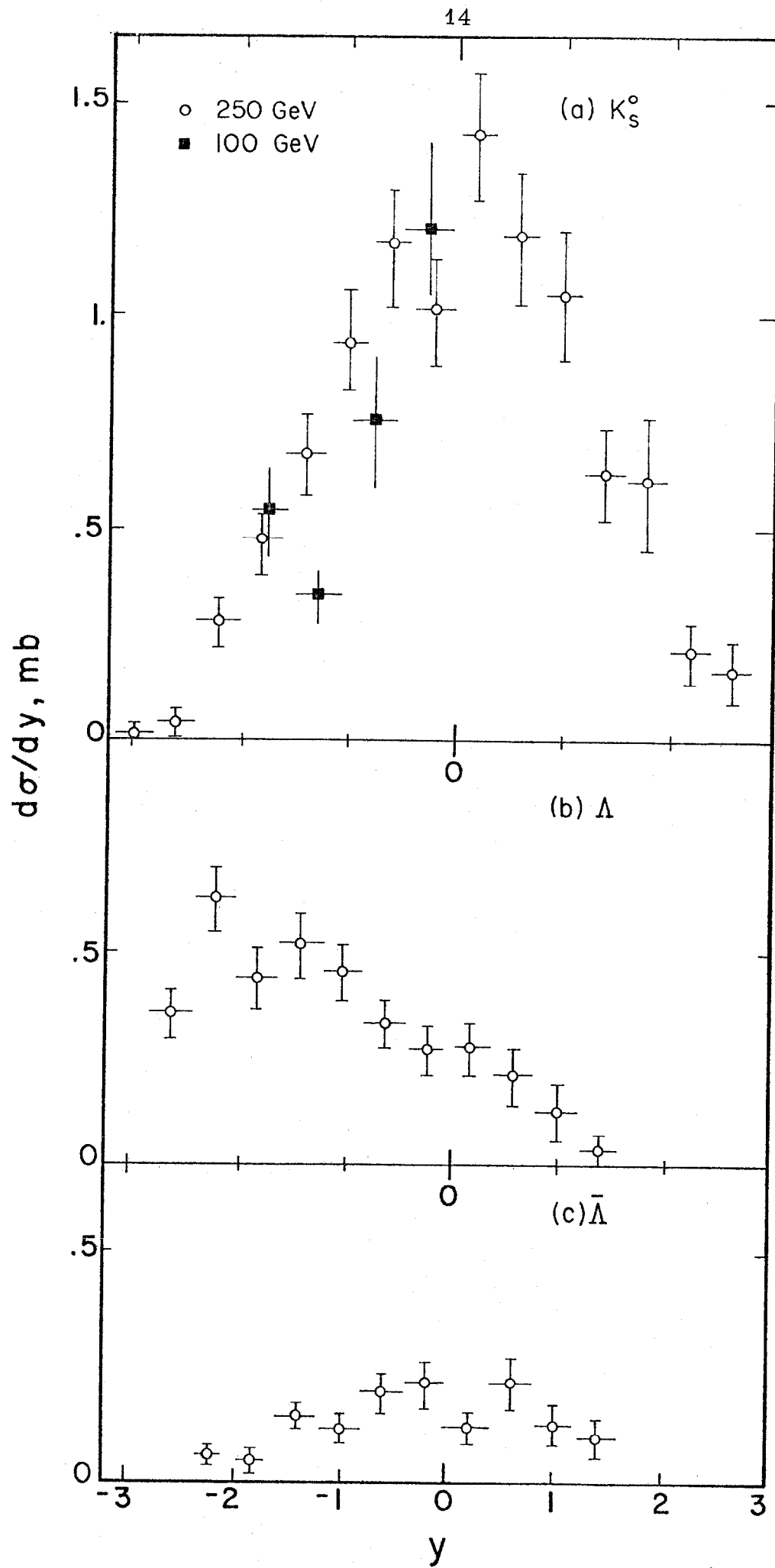


Figure 2

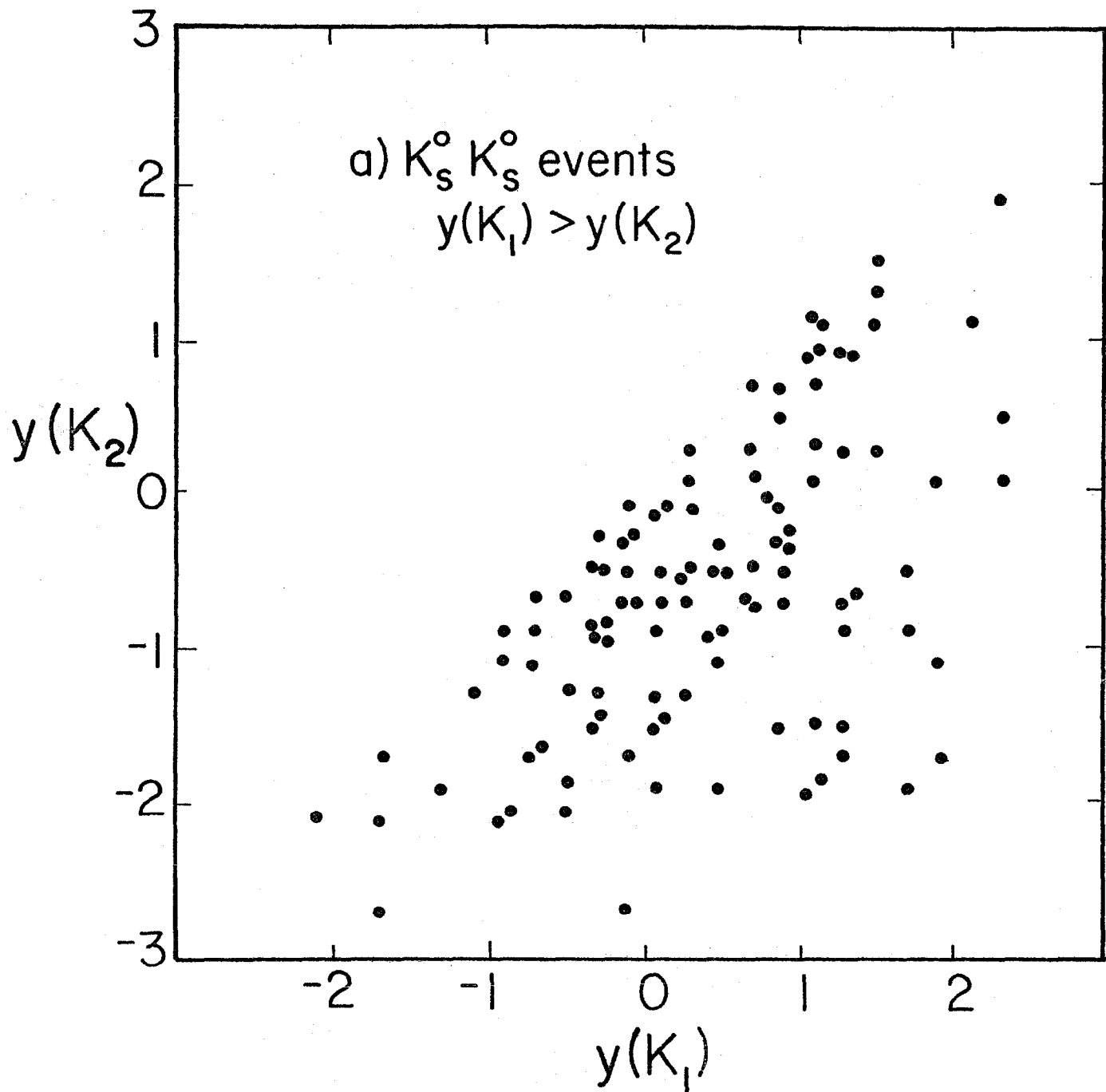


Figure 3a

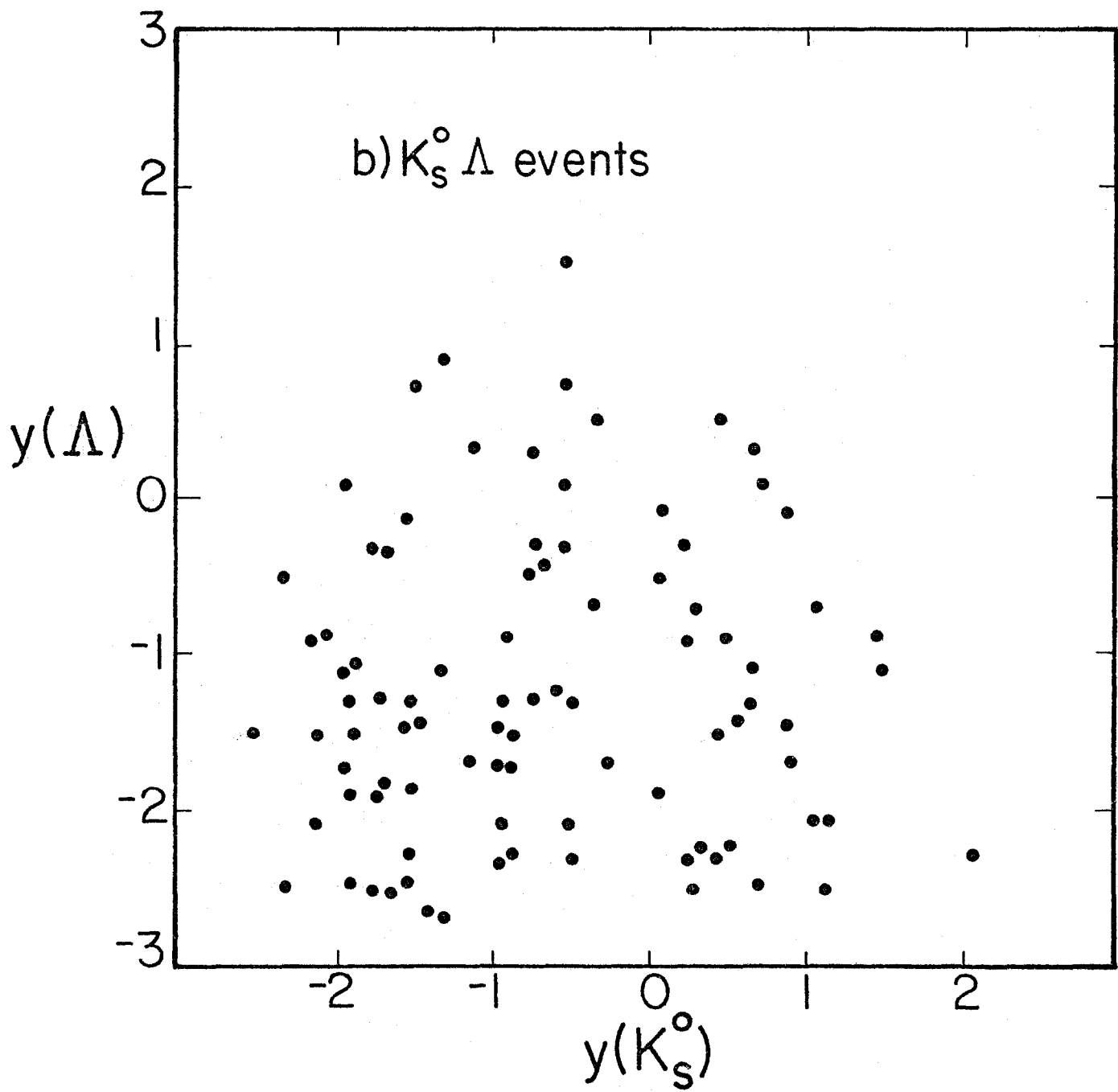


Figure 3b

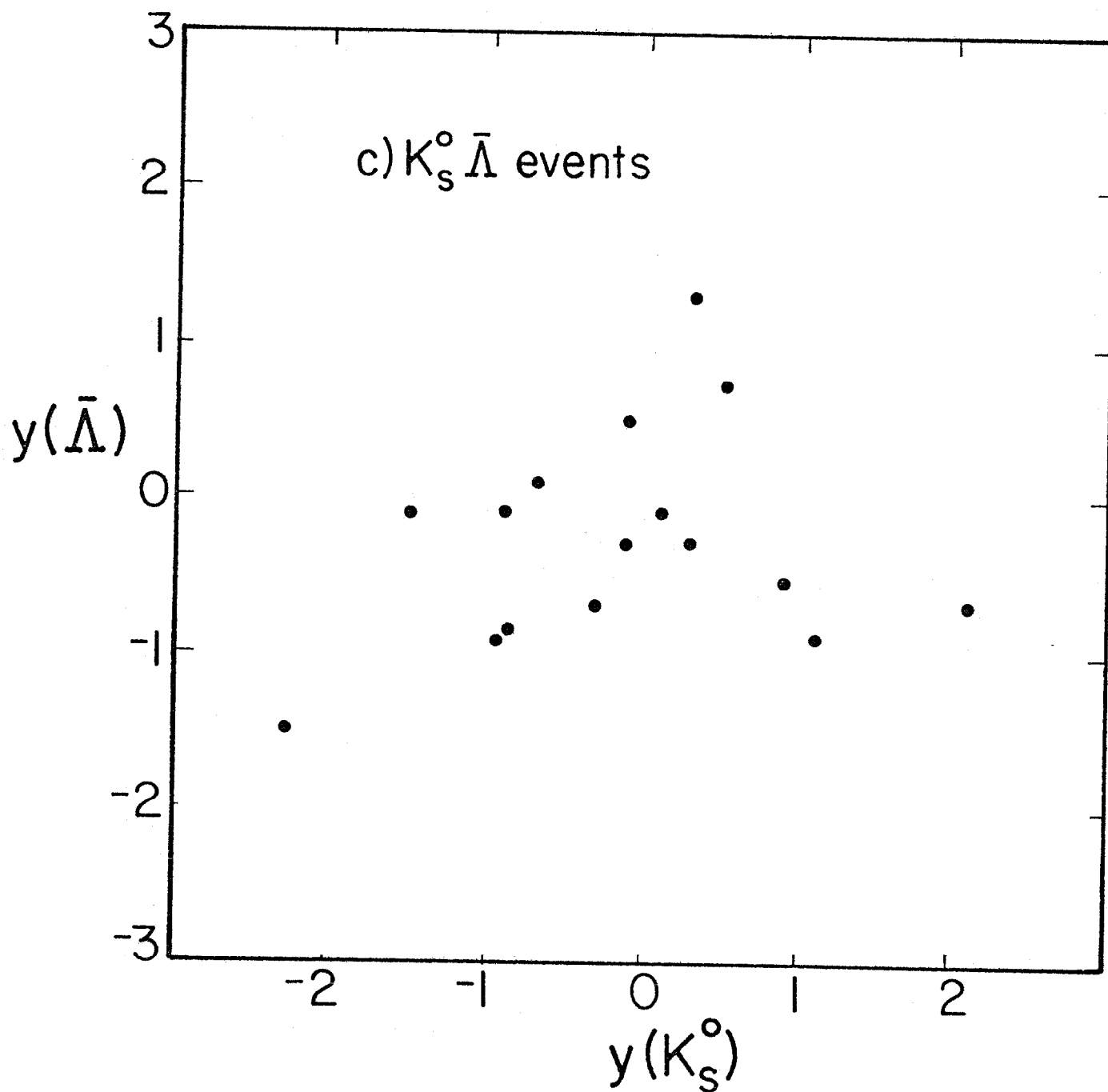


Figure 3c

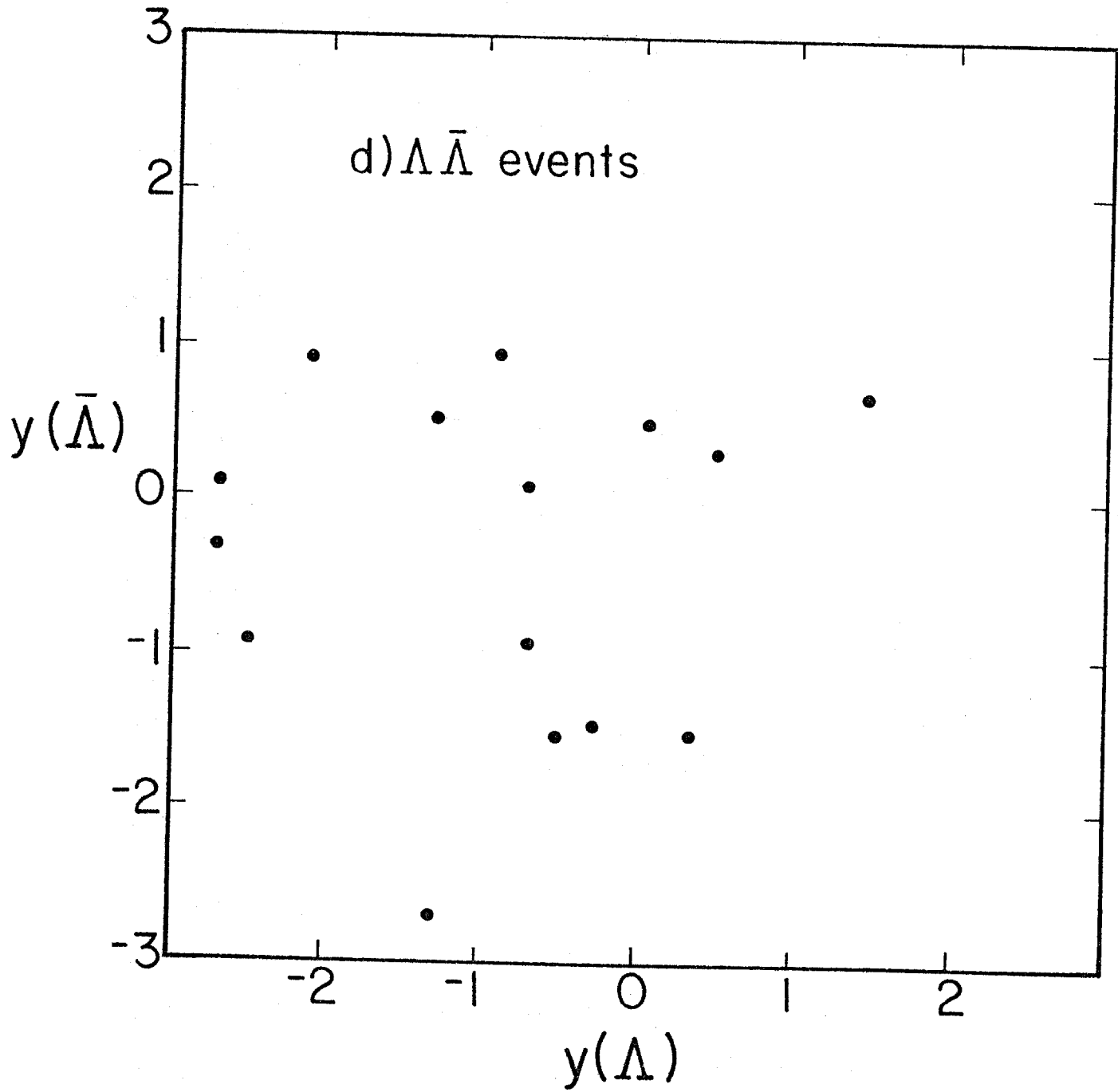


Figure 3d

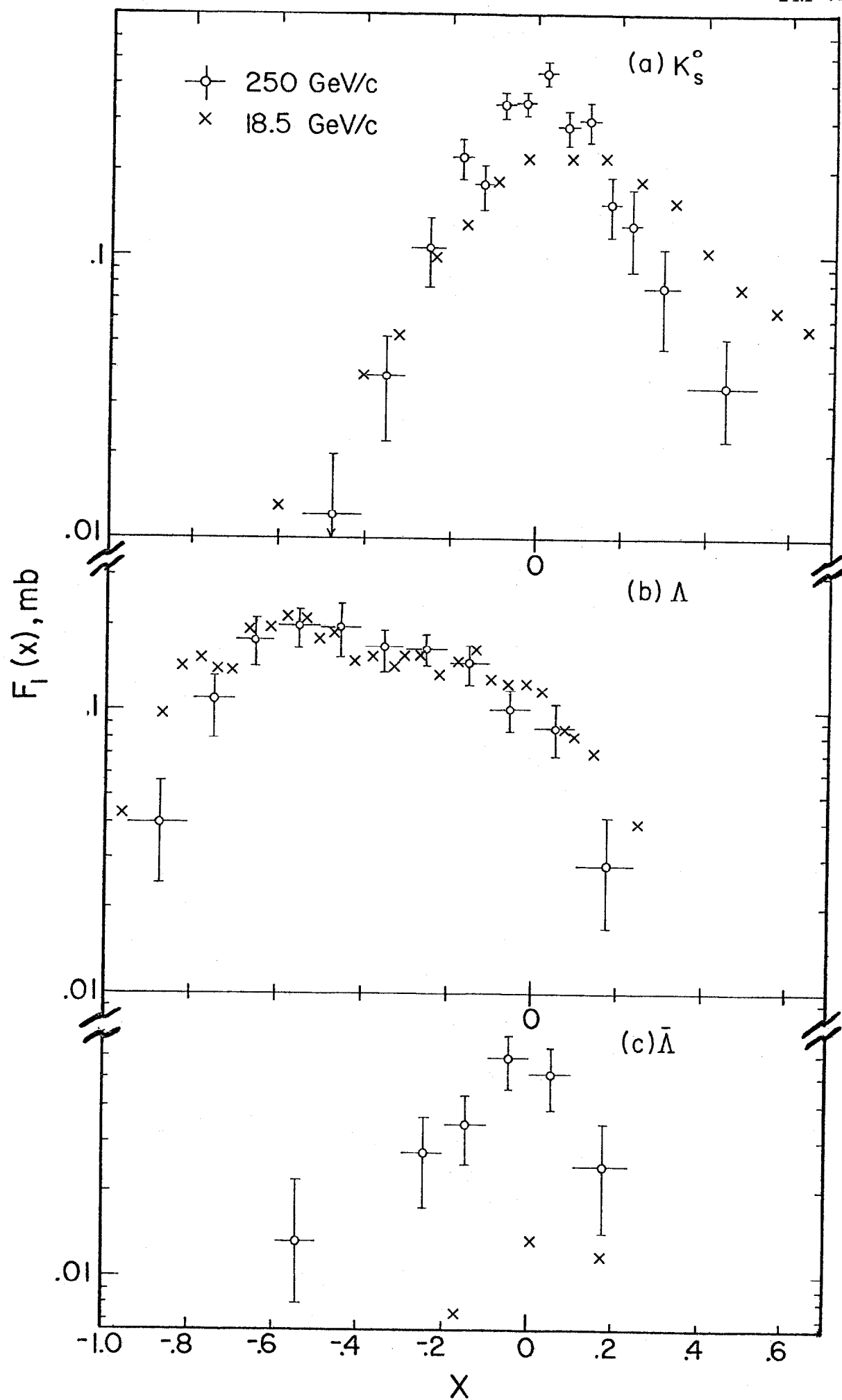


Figure 4a, b, c

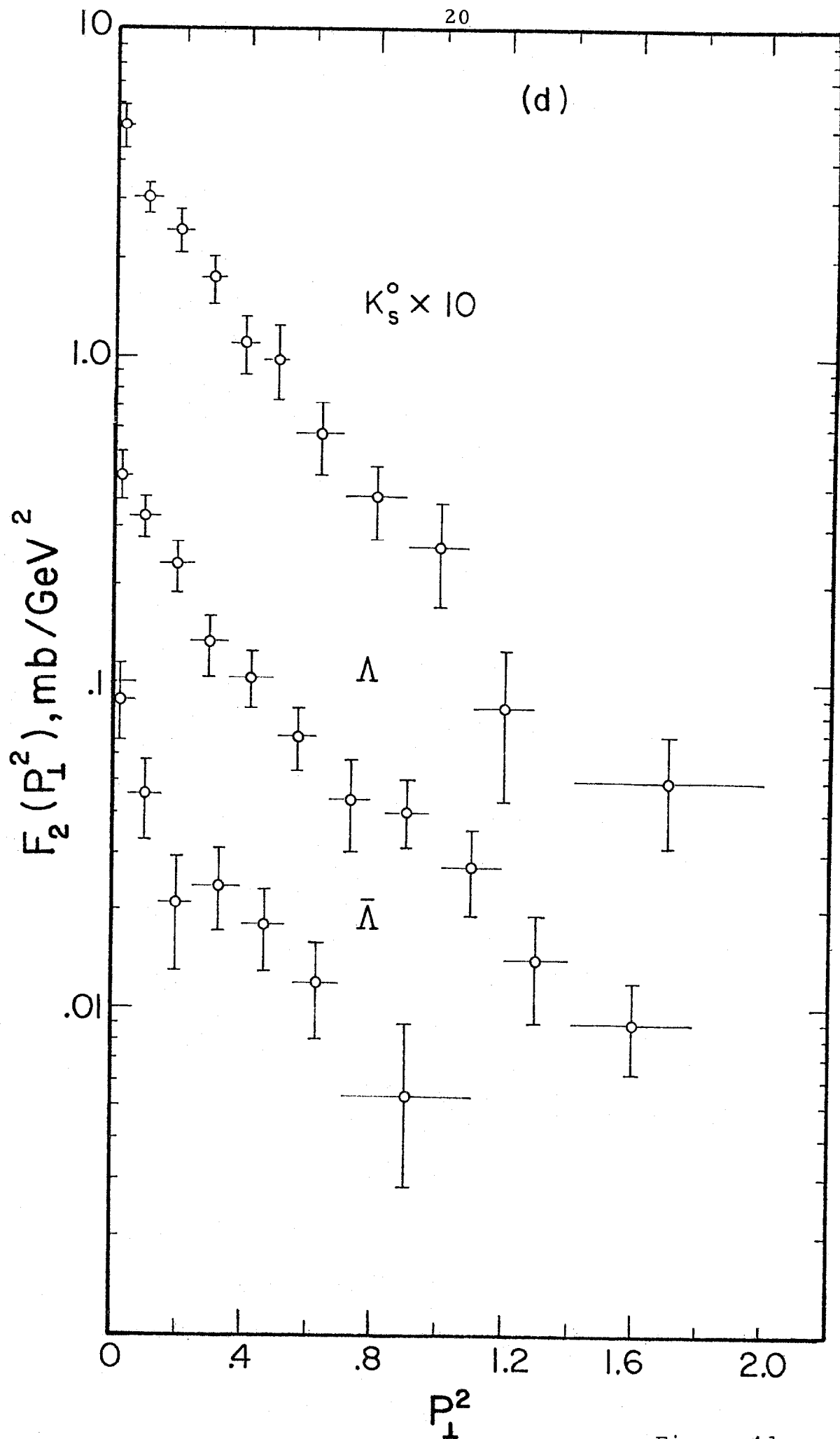


Figure 4d

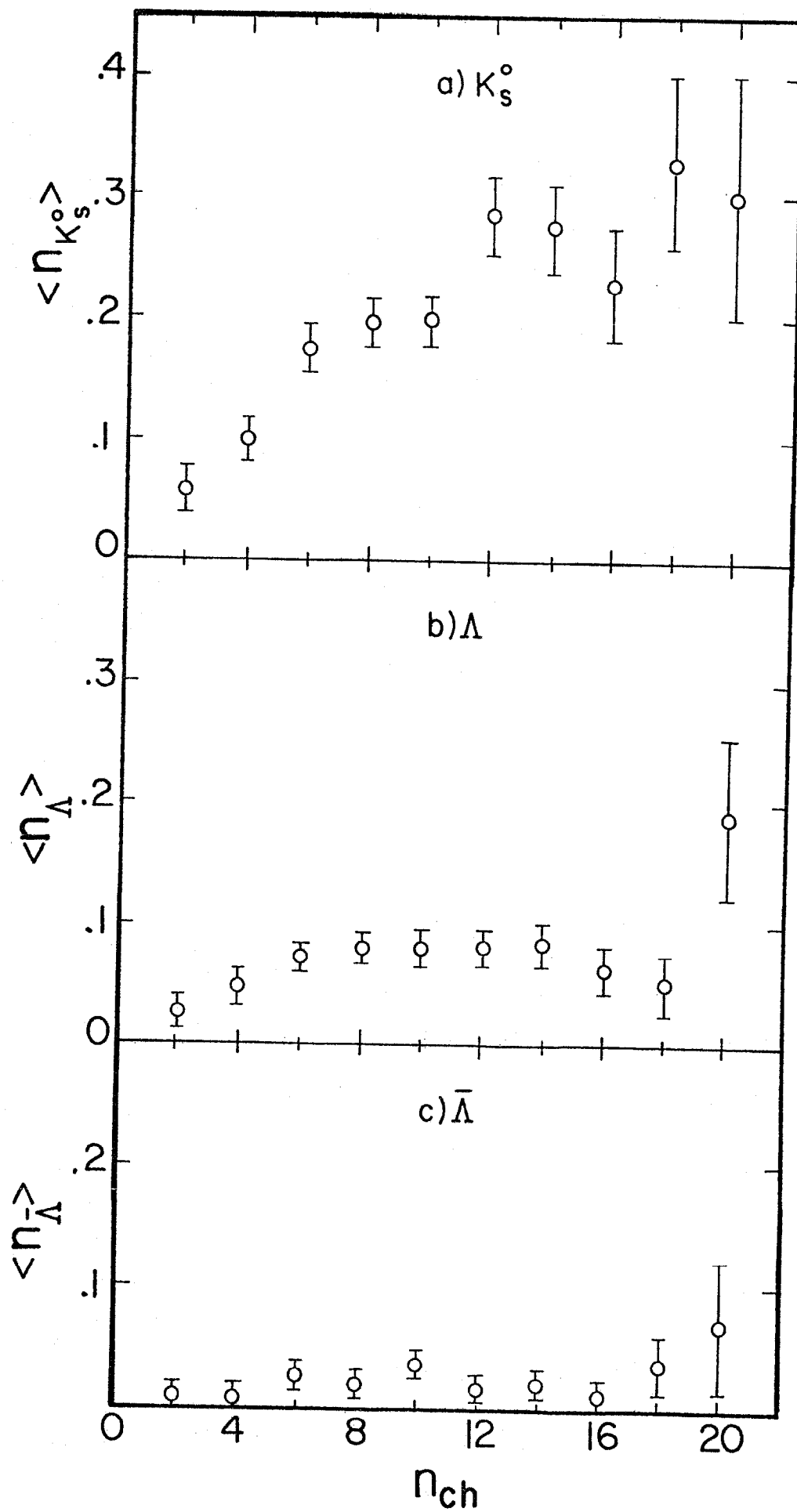


Figure 5a, b, c

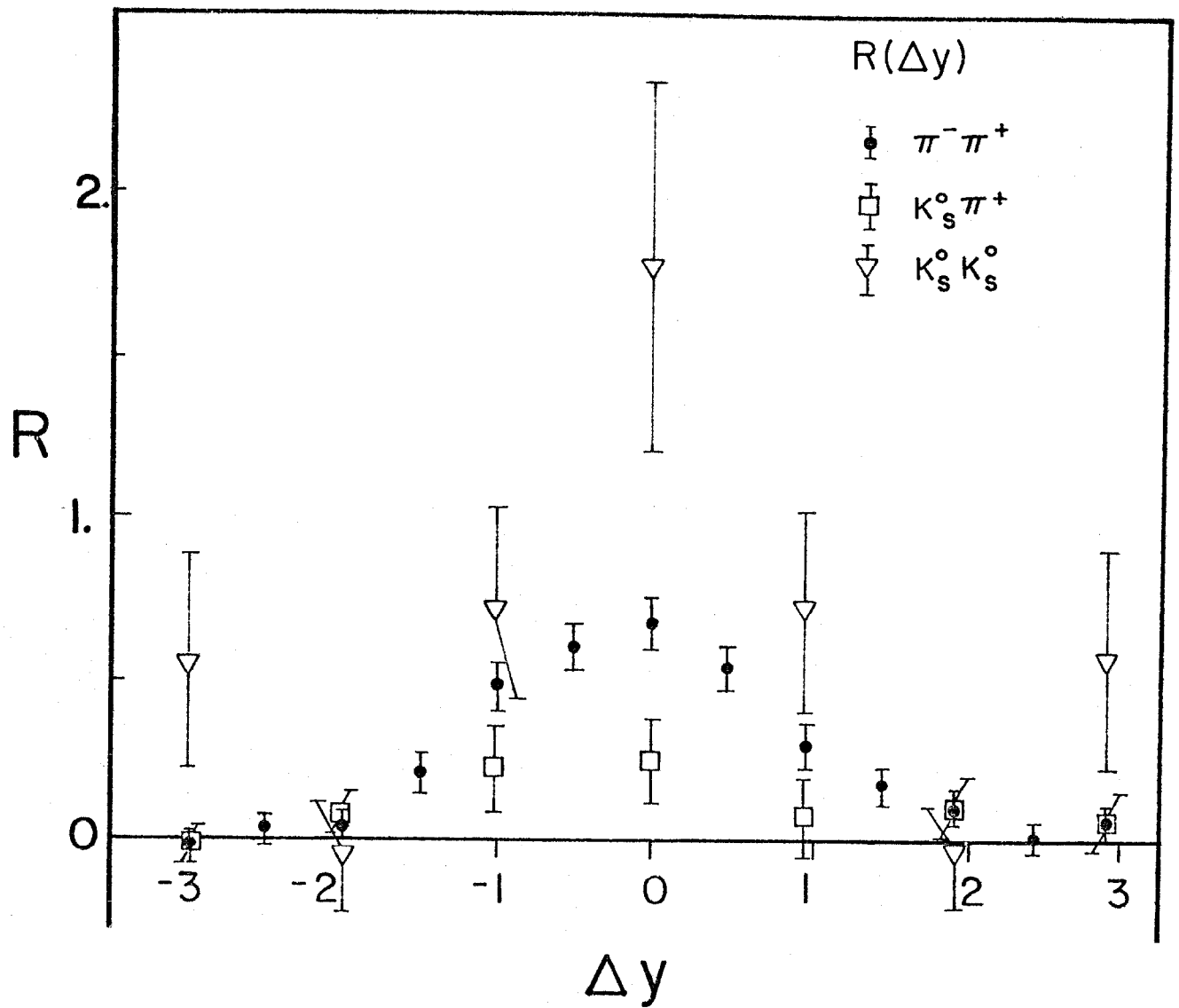


Figure 6